JOURNAL OF MATERIALS SCIENCE **38** (2003) 3979–3993

Formation of translucent hydroxyapatite ceramics by sintering in carbon dioxide atmospheres

J. E. BARRALET*, G. J. P. FLEMING, C. CAMPION, J. J. HARRIS
Biomaterials Unit, School of Dentistry, University of Birmingham, B4 6NN, UK
E-mail: j.e.barralet@bham.ac.uk

A. J. WRIGHT
Chemical Sciences, University of Birmingham, B15 2TT, UK

Hydroxyapatite is used in a variety of clinical applications as a result of the apparent adherence to and mild reaction of bone and soft tissue to it owing to its structural similarity with bone mineral. Transparent hydroxyapatite has previously been fabricated by either or both of two methods; namely the application of pressure during sintering and/or the use of fine particle sized apatite prepared by either a sol-gel process or aqueous precipitation. Recently it has been shown that translucent carbonate hydroxyapatite may be formed by sintering nanocrystalline gels of carbonate hydroxyapatite in a wet carbon dioxide atmosphere. In this study we report for the first time that this atmosphere can be used to sinter microcrystalline powder compacts of hydroxyapatite to form translucent ceramics at ambient pressure. The effect of water partial pressure and sintering time at 1300°C on the optical transmission and microstructure of the ceramic was investigated. It was found that translucent ceramics were formed in all carbon dioxide atmospheres and that optical transmission varied with sintering time. Maximum transmission (~13%) of 2 mm thick ceramic was obtained in materials sintered for four hours at 1300°C in a mixture of carbon dioxide containing water at a partial pressure of 4.6 kPa.

1. Introduction

Hydroxyapatite (HA) has a variety of clinical uses as well as fluorescence and sensor applications. Both bone and soft tissue to can adhere to HA and it is structurally similar to bone and tooth mineral. Bone mineral differs from stoichiometric sintered HA in being nanocrystalline and containing a variety of ionic substitutions, the most abundant being carbonate and sodium [1]. Since HA was first sintered [2, 3] a large number of studies have been performed in order to determine the effects of a variety of initial parameters such as crystallinity [4], agglomeration [5], stoichiometry [6] and substitutions [7] on the physical properties and microstructure of the resulting HA ceramic. As a result of its osteoconductivity, a number of researchers have investigated sintering as a route to producing HA monoliths with highly interconnected macroporosity for bone graft and cell delivery applications [8, 9]. Sintered HA is generally considered to be non-resorbable *in vivo* and linear dissolution rates of approximately 1 μm per year have been reported [10]. In addition to orthopaedic applications, apatite is widely used as a substrate on which to study bone cell behaviour and has also been evaluated in fluorescence and sensor applications [11–15], for which the optical properties can be of importance. Transparent hydroxyapatite has been used to fabricate cell culture dishes and percutaneous devices for monitoring vascularisation *in vivo* [16, 17].

Previous workers have succeeded in fabricating transparent hydroxyapatite by one or a combination of two methods. The application of pressure during sintering, usually by hot isostatic pressing, has resulted in the formation of both transparent and translucent ceramics [18]. Additionally the use of fine particle sized apatite prepared by either a sol-gel process or aqueous precipitation [3, 19] may also yield ceramics displaying optical transmission, whilst the combination of the techniques may result in transparent HA at temperatures as low as 600°C [20]. Recently it has been shown that translucent carbonate hydroxyapatite (CHA) may be formed by sintering nanocrystaline gels made from agglomerated aqueous sols of CHA in a wet carbon dioxide atmosphere at temperatures of 1000°C [21]. In this study we report for the first time that a carbon dioxide atmosphere can be used to sinter microcrystalline powder compacts of hydroxyapatite to form translucent ceramics at ambient pressure. The effect of water partial pressure and sintering time at 1300°C on the optical transmission and microstructure of the ceramic is also investigated.

*Author to whom all correspondence should be addressed.

2. Methods

2.1. Green body preparation and characterisation

Green powder compacts were produced by pressing 3 g of HA powder, (sintering grade P210, Plasma Biotal, Tideswell, UK) uniaxially at a pressure of 80 MPa in a cylindrical die (25 mm diameter). The green compacts were dried in an oven at 110°C and the mass and dimensions of the pellets were measured.

The phase composition and lattice parameters of the starting powder and sintered HA were characterised using X-ray powder diffraction (Siemens D-5000, $2\theta = 5°–80°$, step, 0.02°, count time 2 s) followed by Rietveld refinement and FTIR spectroscopy (Nicolet 520, KBr disc, wave number 500–4000 cm^{-1}) was used to determine changes in composition. Thermogravimetric analysis (TGA) was performed on a STA1500 Rheometric Scientific Thermal Analyzer. Samples were heated in air to 120°C (held 1 h, to determine adsorbed water) then ramped (10°C min^{-1}) to 1400°C and held until no further weight loss was detectable. FTIR after TGA were employed to confirm the removal of all carbonate.

2.2. Sintering

Sintering of the HA green compacts ($n = 6$) was performed at 1300°C (Lenton 1500°C Vacuum Tube Furnace) for different times; namely 0, 0.5, 2, 4, 8 and 24 h, using a heating and cooling rate of 5°C min^{-1}. Carbon dioxide with varying water vapour partial pressures was used as the furnace atmosphere. Different water vapour partial pressure was achieved by flowing carbon dioxide (1 litre min^{-1}) at 22°C through double distilled water or saturated solutions of either potassium acetate or di-sodium orthophosphate, since saturated solutions of these compounds are known to affect the water vapour pressure of air in equilibrium with the solutions [22], to determine whether control of furnace atmosphere could also be obtained under non-equilibrium conditions using this relatively simple method. The dynamic shrinkage during sintering was determined by dilatometry (Netzsch 402E) using the same heating regime and atmospheres as used in the tube furnace for sintering experiments.

2.3. Ceramic characterisation

The densities of the sintered pellets were determined using helium pycnometry (Micromeritics AccuPyc 1330). Optical transmission of 2 mm thick sintered HA ground with 320 grit silicon carbide was determined using a dental curing light (Heliomat H2, Vivadent UK) as a light source and a photo-voltaic detector (303–674, RS Components, UK) as a detector. Setting C of the curing light was used as this gave the narrowest distribution of wavelengths and hence the most monochromatic light source (~530 nm) as shown in Fig. 1. The current/intensity relationship was determined by measuring the current of the transmission experimental configuration in the absence of a sample and assigning this value as 100%. Intensity was varied to produce a calibration curve from which percentage transmission was calculated.

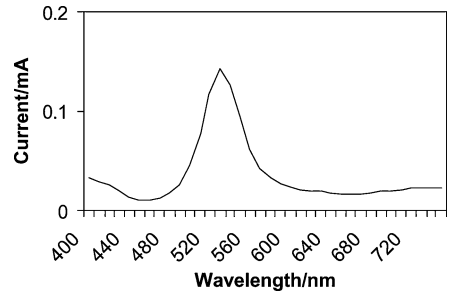

Figure 1 Measured voltage as a function of wavelength of light from Heliomat H2 light source.

Sintered HA ceramic was embedded in epoxy resin (Epofix, Struers, UK) and sections were cut, ground, polished to a 1 μm finish and etched using 0.5% phosphoric acid solution for 60 s. Specimens were then gold coated using a Desk II sputter coater (Denton Vacuum, UK) for 40 s. The microstructure of the sintered HA was examined by scanning electron microscopy (JEOL JSM-5300LV). Images of grain boundaries for image analysis were obtained using an accelerating voltage of 30 kV, working distance of 12 mm and stage tilt of 10°. 32-Bit images were recorded at a resolution of 1976 × 1475 pixels and were re-sampled at 8-bit at 800 × 600 pixels. Subsequent analysis of images was carried out using Optimas image analysis software (Media Cybernetics, LP, USA), calibration of the software against the SEM having been carried out by means of a TEM grid of known dimensions. The number of pores mm^{-2} was calculated from representative electron micrographs and average maximum pore dimension of at least 60 pores (where sufficient pores could be found) was measured manually. Grain size was measured by linear intercept as the average of at least 80 grains from images recorded at 20 kV accelerating voltage and a working distance of 12 mm from gold coated etched, ground and polished, flat samples.

3. Results

The average water partial pressures of humidified furnace gasses were estimated by measuring the weight loss of the humidifying solutions before and after experimentation and by calculating the volume of carbon dioxide passed through the solutions. It was assumed that 1 mole of carbon dioxide or water vapour occupied 24 litres and that the water content of the gas was constant throughout the experiment. The water content of the carbon dioxide, as stated by the manufacturer (BOC Gases, UK), was 7 ppm. The water contents of carbon dioxide saturated with water and various saturated solutions are shown in Table I.

The XRD pattern indicated that within the limits of the technique (>5%) the starting powder was a phase pure hydroxyapatite. FTIR spectroscopy revealed the presence of a small quantity of carbonate as indicated by two peaks at 1446 and 1418 cm^{-1}. Manufacturer's data indicated that the carbonate content of the powder was 2.8%. The mean relative density of the green compacts was 46 ± 2% as calculated from mass and dimension measurements.

TABLE I Water partial pressure of carbon dioxide gas passed through various humidifying solutions

CO_2 humidifying solution	Water partial pressure (kPa)
None	0.0007
Saturated potassium acetate	2.5 ± 0.9
DDW	3.2 ± 0.4
Sodium orthophosphate solution	4.6 ± 0.9

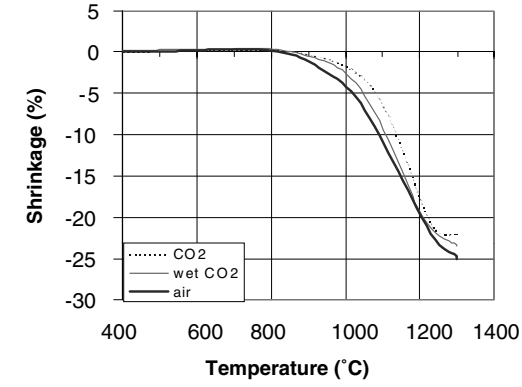

(a)

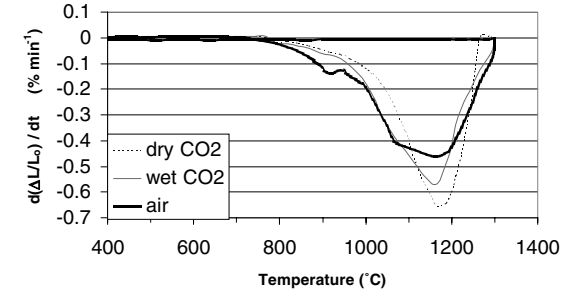

(b)

Figure 2 Dilatometry (a) shrinkage and (b) derivative plots of HA powder compacts heated to 1300°C at 5°C min^{-1}.

3.1. Dilatometry

The shrinkage of the compacts during sintering in air, carbon dioxide and carbon dioxide with 3.2 kPa water vapour is shown in Fig. 2a. HA sintered in carbon dioxide alone appeared to begin densification at approximately 30°C higher than HA sintered in air or carbon dioxide and water mixture which both commenced densification at approximately 790°C. Densification of HA sintered in carbon dioxide was complete at around 1260°C, whereas when sintered in air, densification was complete after 18 min dwell at 1300°C. In contrast, HA sintered in the water/carbon dioxide mixtures ceased densification within the first five minutes of the dwell cycle. As determined from the derivative plot of shrinkage against time between 1100 and 1200°C the shrinkage rate of HA was fastest in carbon dioxide atmosphere and slowest in air (Fig. 2b). The rate of shrinkage was greatest at a temperature of ∼1180°C in all atmospheres investigated. The temperature of the maximum magnitude for the rate of change was increased by the presence of carbon dioxide and the onset of significant change was increased to a higher temperature. However the presence of water vapour reduced both the onset temperature and the maximum magnitude of the change.

3.2. Pycnometry

The change in percentage relative density as measured by helium pycnometry of the HA with dwell time in the atmospheres investigated is shown in Fig. 3. Theoretical density was assumed to be 3.156 Mg m^{-3} [3]. After a temperature ramp up to 1300°C followed by a ramp down in temperature with no dwell cycle, all the specimens had densities between 98.4 and 99.4%. As dwell time increased from 0 to 24 h, the density of HA sintered in carbon dioxide appeared to decrease from 99.35 to 98.35%. At all sintering times investigated HA sintered in air had a lower apparent density than HA sintered in carbon dioxide containing water vapour. Variation in the water content of the carbon dioxide atmosphere had little effect upon the density of HA at dwell times greater than 0 h.

3.3. Microstructure

Except after a sintering regime with no dwell, HA sintered in air had a significantly smaller grain size than HA sintered in carbon dioxide atmospheres and was

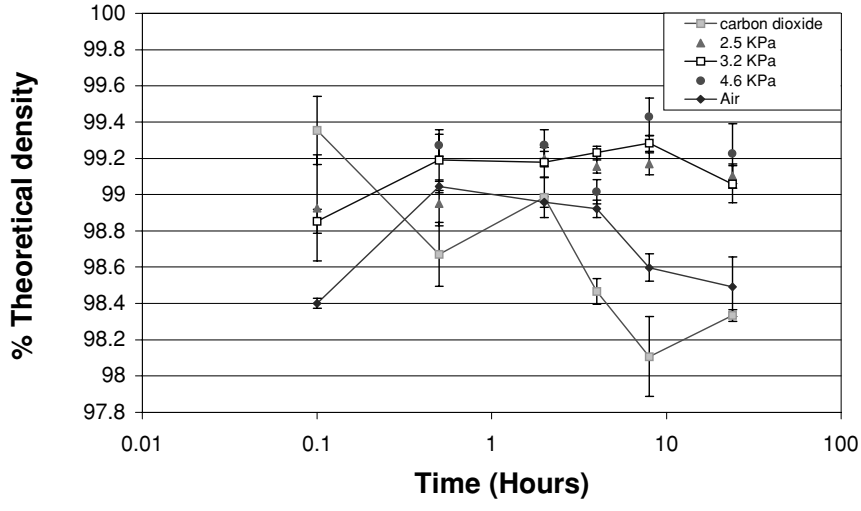

Figure 3 Effect of sintering time and atmosphere on the relative density of HA ceramics.

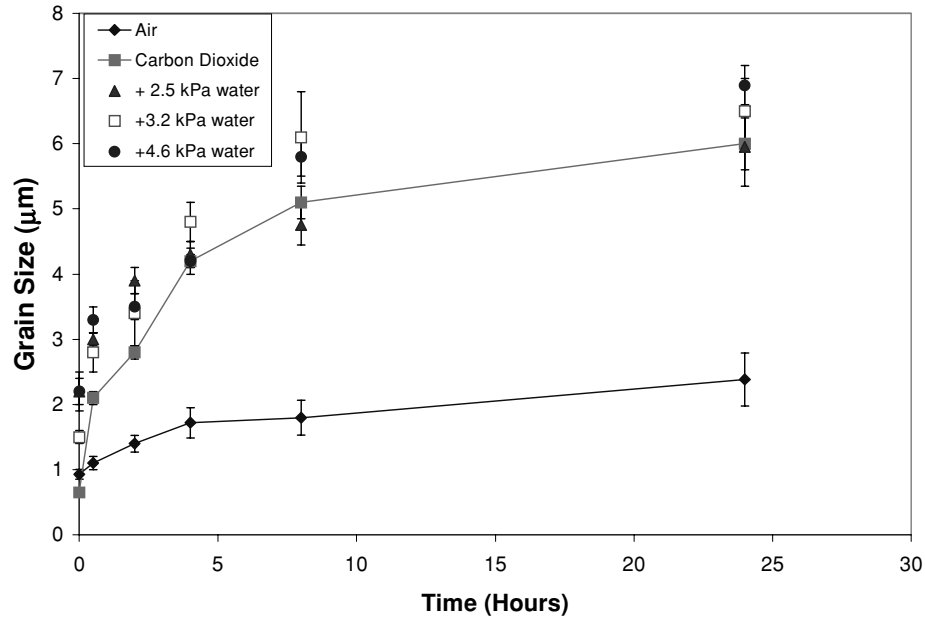

Figure 4 Effect of sintering time and atmosphere on the grain size of HA ceramics.

2.4 μm after a twenty-four hour dwell compared with 6–7 μm after sintering in carbon dioxide atmospheres. HA sintered in wet carbon dioxide atmospheres generally had larger grain sizes than HA sintered in carbon dioxide alone especially at dwell times less than 8 h, (Fig. 4).

Fig. 5a–d show the microstructures of HA sintered in air at 1300°C for 0, 2, 4 and 24 h respectively. Porosity was predominantly intergranular and located at triple points, whereas at the same conditions in carbon dioxide (Fig. 6a–d) some intragranular porosity was apparent after a heating and cooling regime with no dwell (Fig. 6a). However after sintering for 2, 4 and 24 h in dry carbon dioxide the microstructure was essentially pore free (Fig. 6b–d). When sintered in an atmosphere of carbon dioxide and 3.2 kPa water partial pressure at 1300°C, both inter and intragranular porosity was evident after sintering for 0 and 2 h (Fig. 7a and b) whereas after sintering at longer times, i.e., 4 and 24 h only intragranular porosity was observed (Fig. 7c and d).

3.4. Grain size distribution

The grain size distributions of HA sintered at 1300°C in air, carbon dioxide and water/carbon dioxide are shown in Fig. 8a–c respectively. Some data were removed for clarity. It can be seen that the modal value of the grain size of HA sintered in air increased only after sintering at times of more than 8 h (Fig. 8a), whereas after only 0.5 h sintering time in carbon dioxide, grain growth could be observed as indicated by the peak in grain area histogram at 4 μm^2 in Fig. 8b. However when sintered in a 3.2 kPa water and carbon dioxide mixture, the modal grain size did not change until after 2 h sintering (Fig. 8c). At sintering times longer than this, a broad peak between 20 and 30 μm^2 was observed indicating that grain coarsening had occurred.

3.5. Pore size

Sintering atmosphere had a large effect on pore size and pore density as shown in Table II. When sintered for up to four hours in air, detected pores were submicron in dimension and were present at comparatively high densities (3–7 $\times$ 10^4 mm^{-2}). However in carbon dioxide atmospheres, pores were present at a lower density (0.3–2 $\times$ 10^3). The presence of 3.2 kPa water in the carbon dioxide sintering atmosphere appeared to increase pore density and reduce pore size after sintering for up to 4 h. After twenty-four hours sintering, in contrast with HA sintered in dry carbon dioxide, average pore size decreased as only intragranular porosity was observed.

3.6. Optical transmission

All ceramics were blue in colour and this was thought to be due to a change in oxidation state of transmission metal ion impurities. Optical transmission at 530 nm of

TABLE II Effect of sintering atmosphere and time on pore size and density (mean (sd))

	Air		Carbon dioxide		Carbon dioxide +3.2 kPa water	
Sintering time (h)	Pore density (No $\times$ 10^3 mm^{-2})	Dimension (mm)	Pore density (No mm^{-2})	Dimension (mm)	Pore density (No mm^{-2})	Dimension (mm)
2	73 (3)	0.5 (0.2)	1800 (500)	0.8 (0.6)	2400 (200)	1.8 (1.3)
4	45 (3)	0.7 (0.3)	500 (130)	4.8 (2.1)	3200 (400)	2.1 (0.9)
24	35 (12)	1.2 (0.6)	460 (20)	6.1 (3.4)	300 (700)	0.5 (0.7)

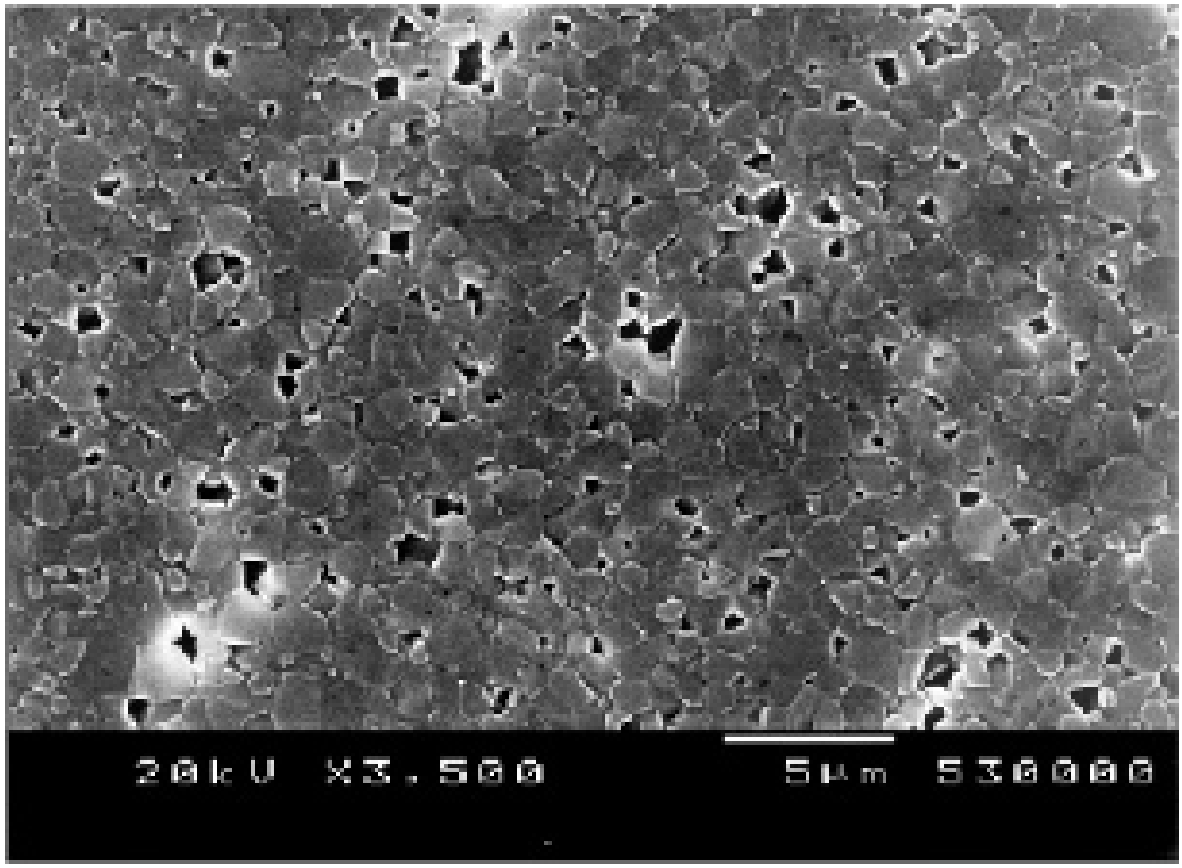

(a)

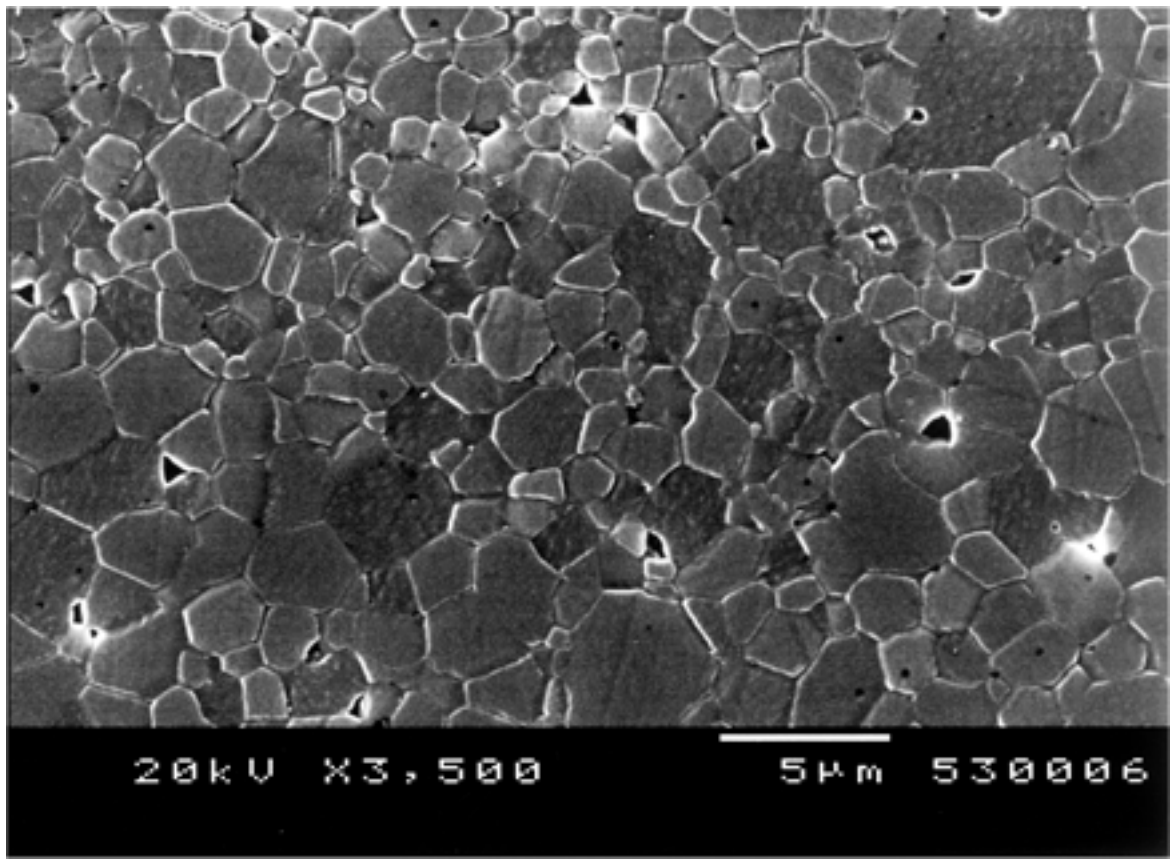

(b)

Figure 5 Microstructures of HA ceramic sintered in air at 1300°C for (a) no dwell, (b) 2, (c) 4, and (d) 24 h. (*Continued*)

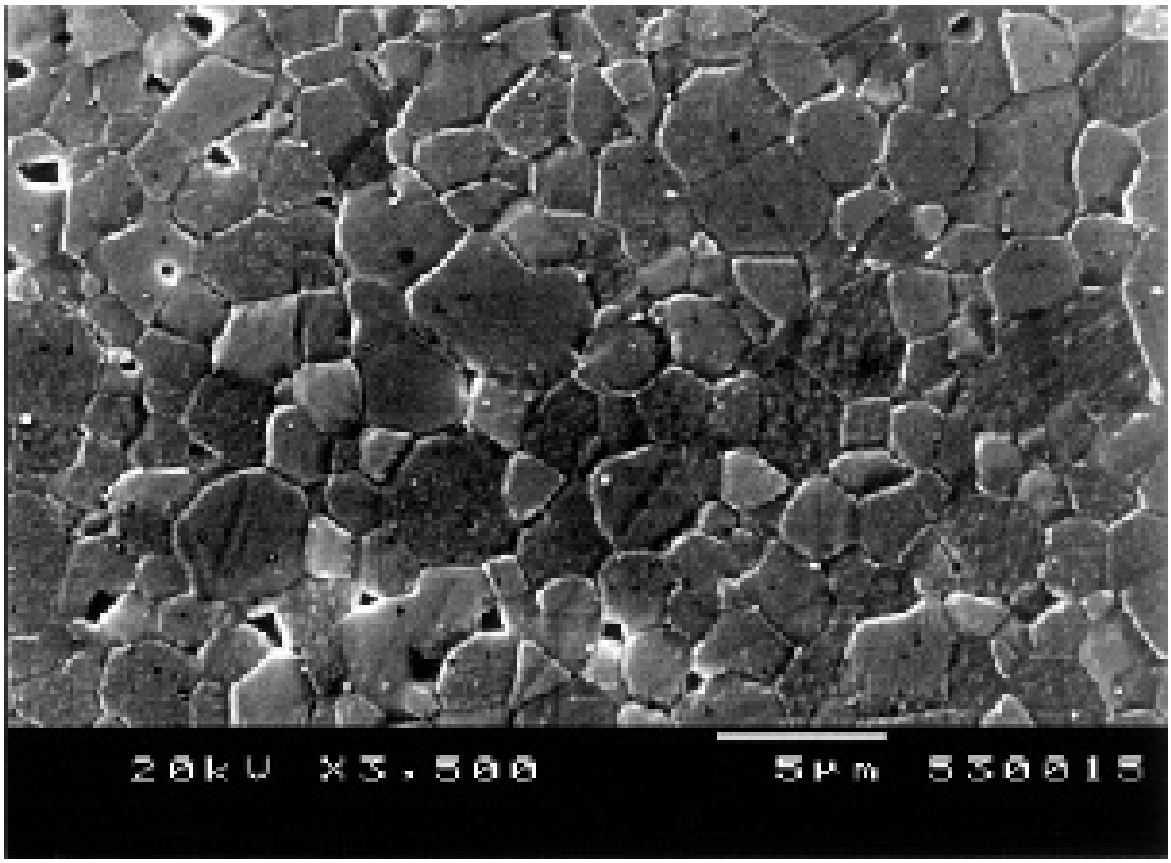

(c)

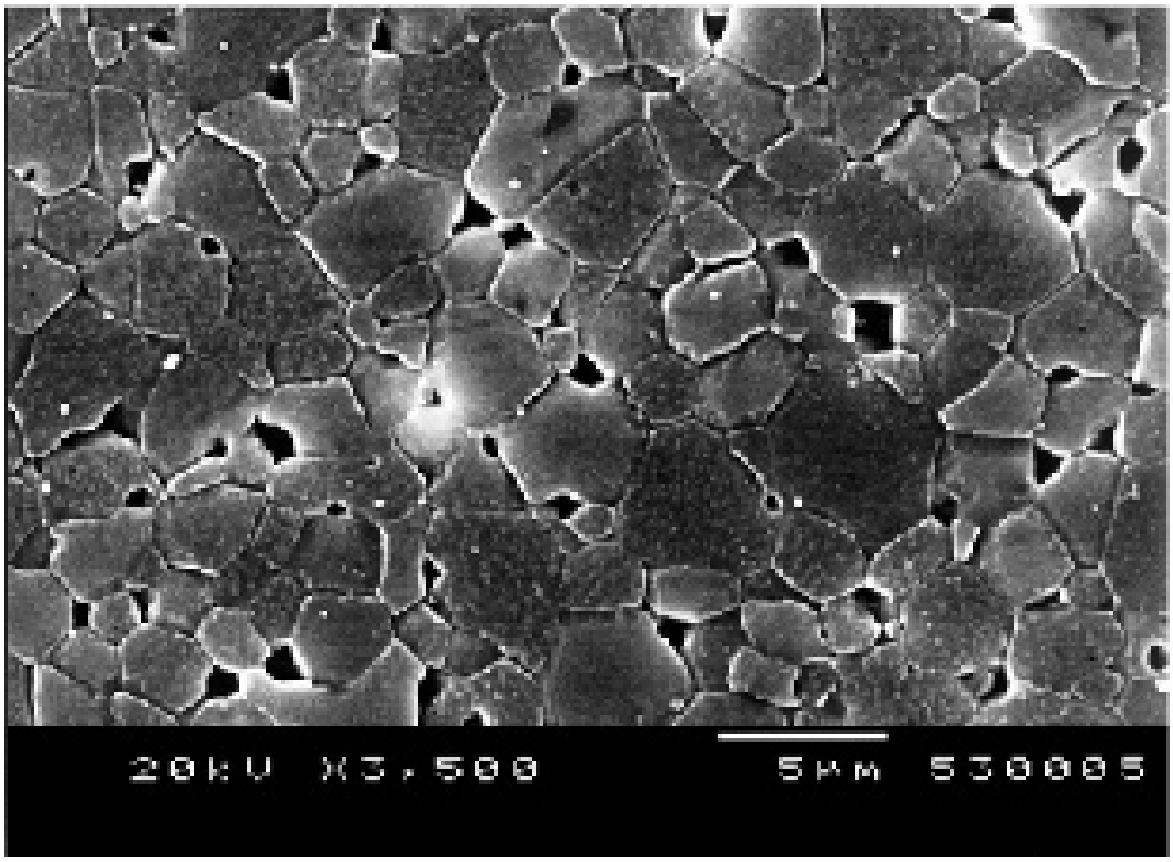

(d)

Figure 5 (*Continued*).

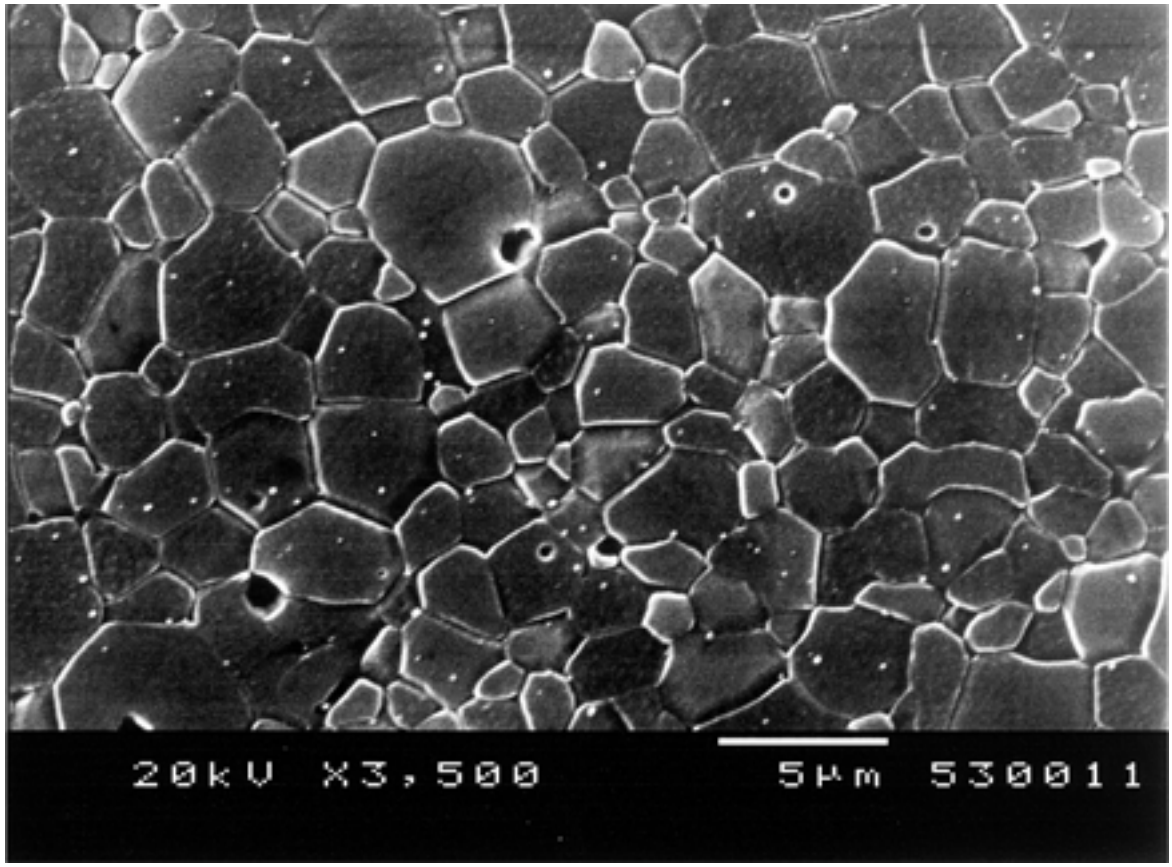

(a)

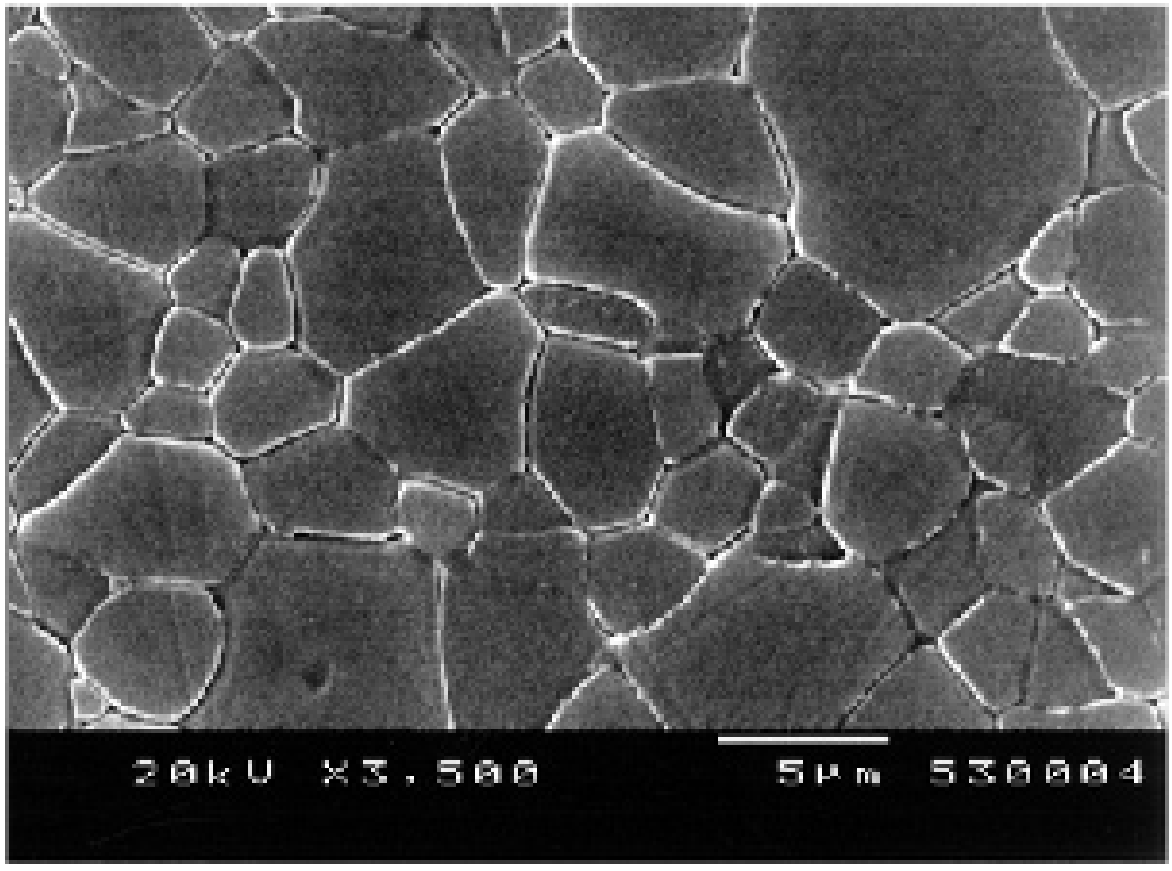

(b)

Figure 6 Microstructures of HA ceramic sintered in carbon dioxide at 1300°C for (a) no dwell, (b) 2, (c) 4, and (d) 24 h. (*Continued*)

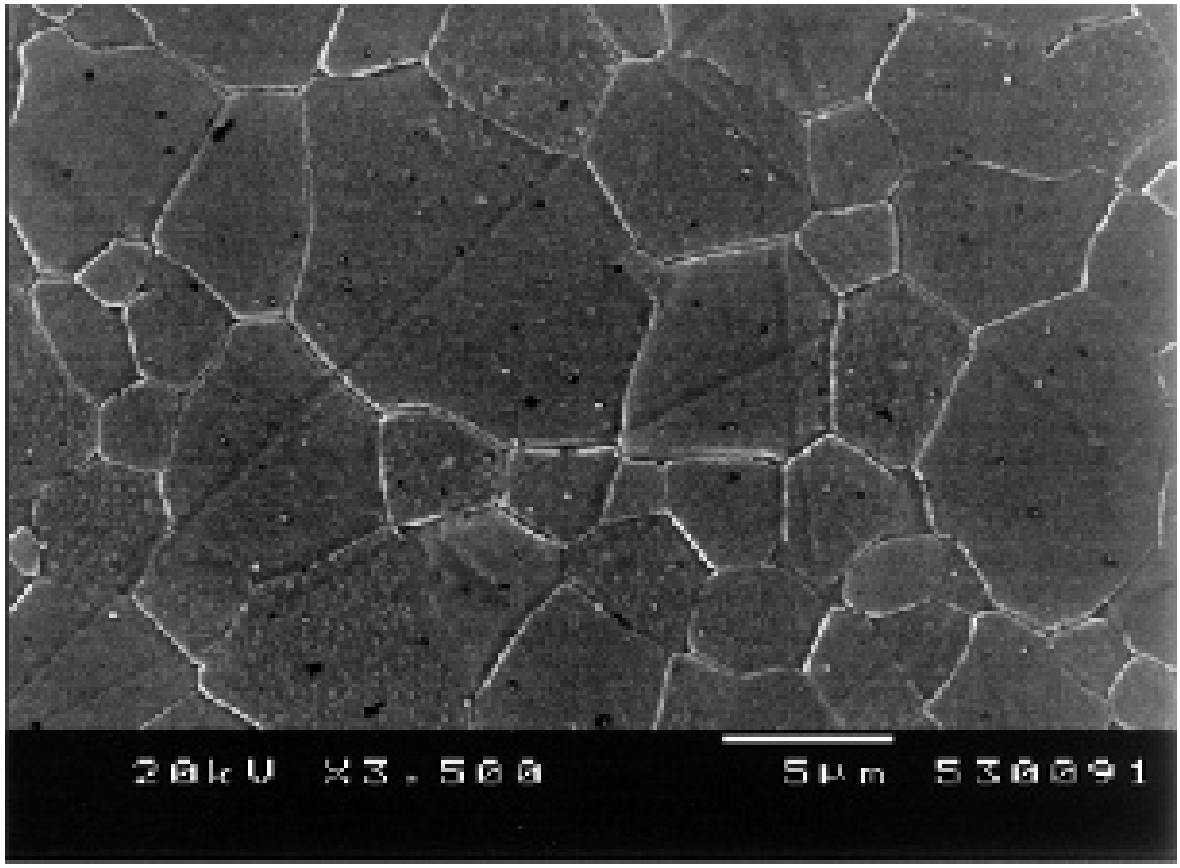

(c)

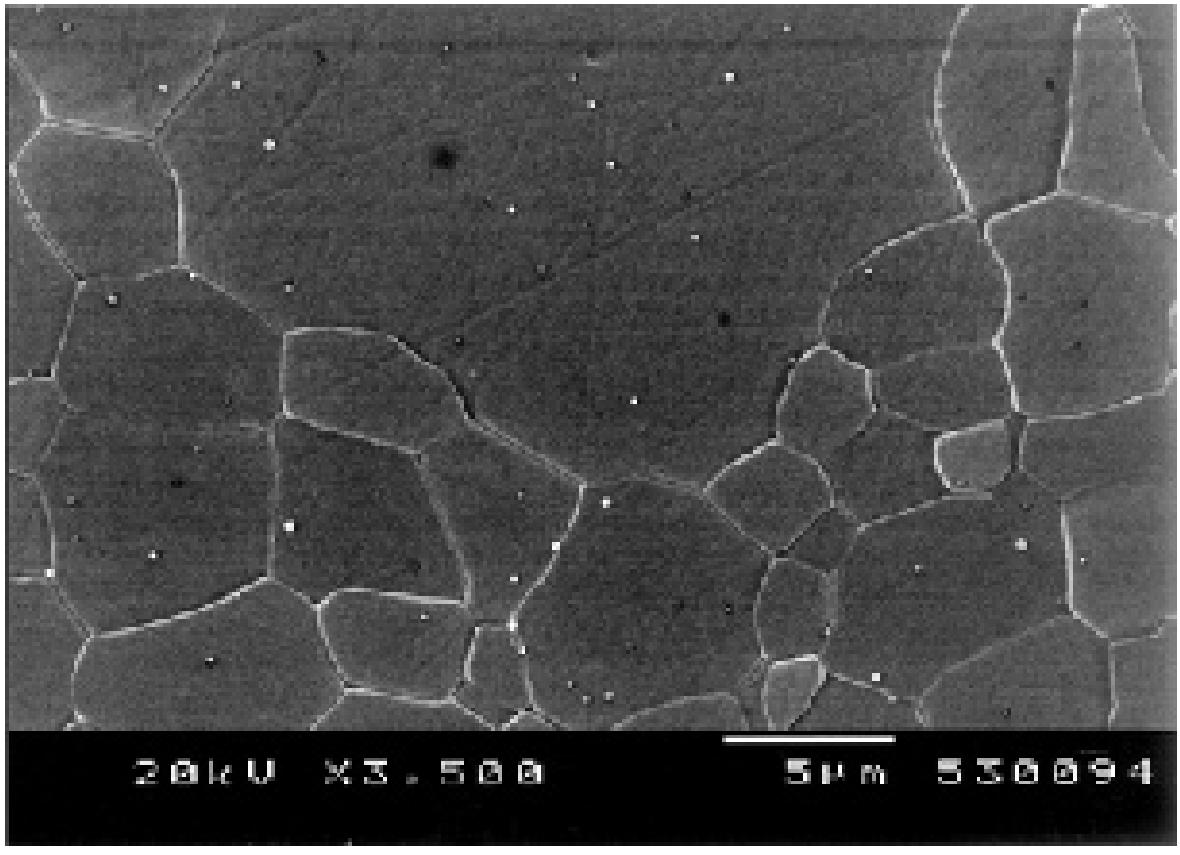

(d)

Figure 6 (*Continued*).

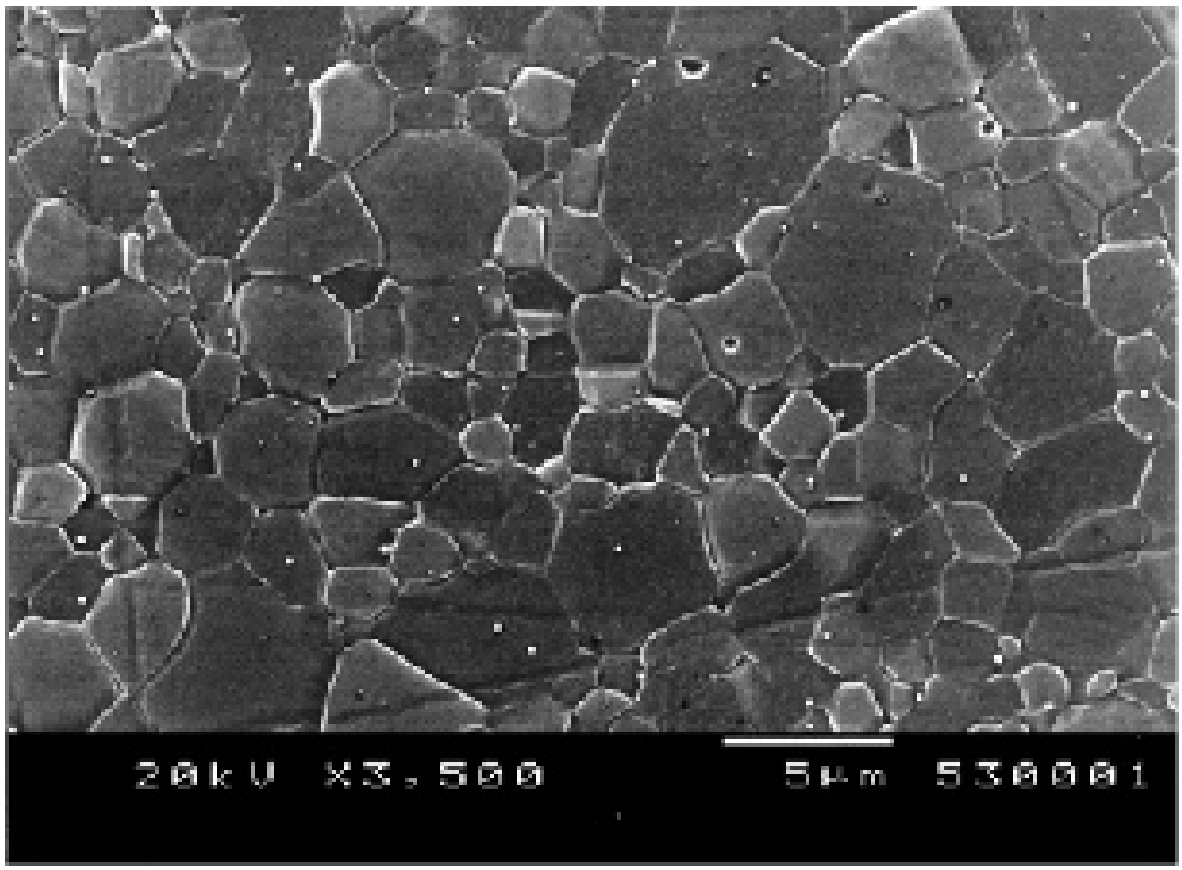

(a)

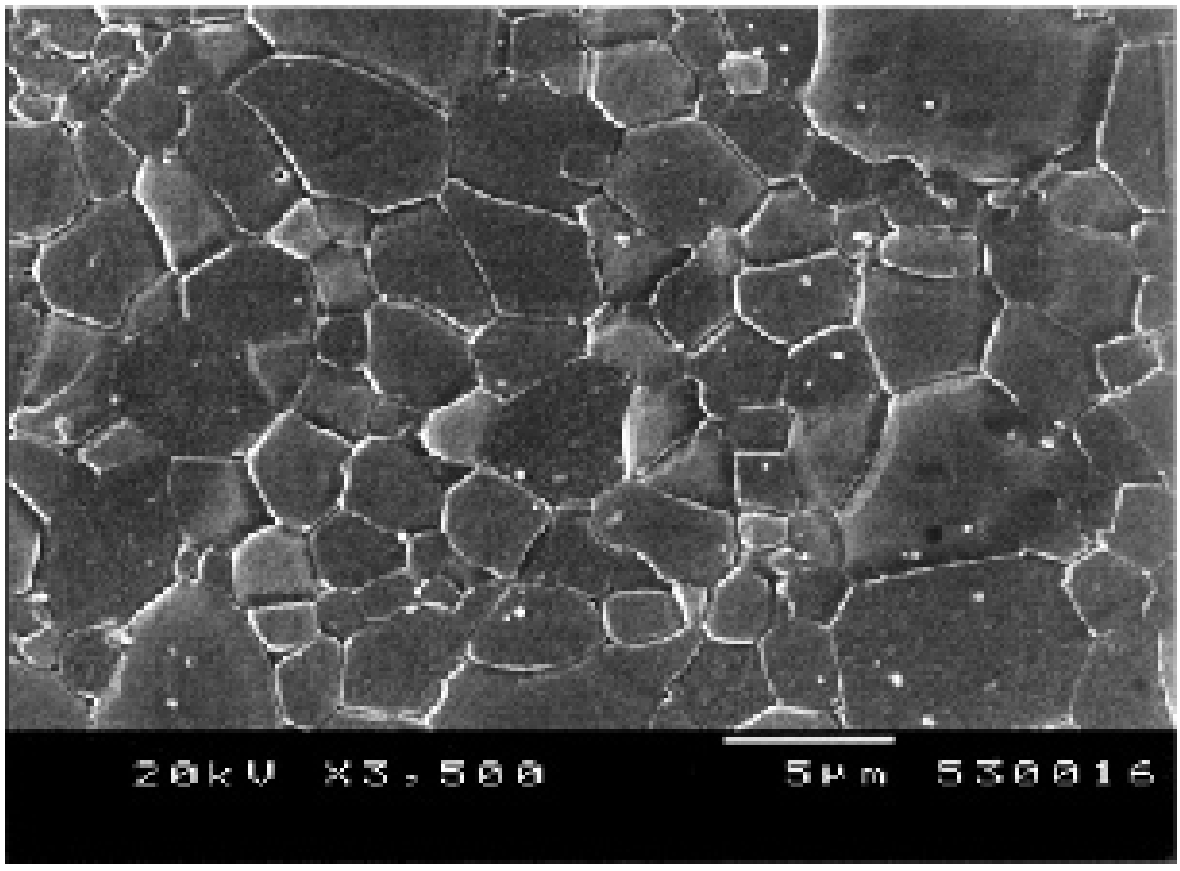

(b)

Figure 7 Microstructures of HA ceramic sintered in carbon dioxide with 3.2 kPa water at 1300°C for (a) no dwell, (b) 2, (c) 4, and (d) 24 h. (*Continued*)

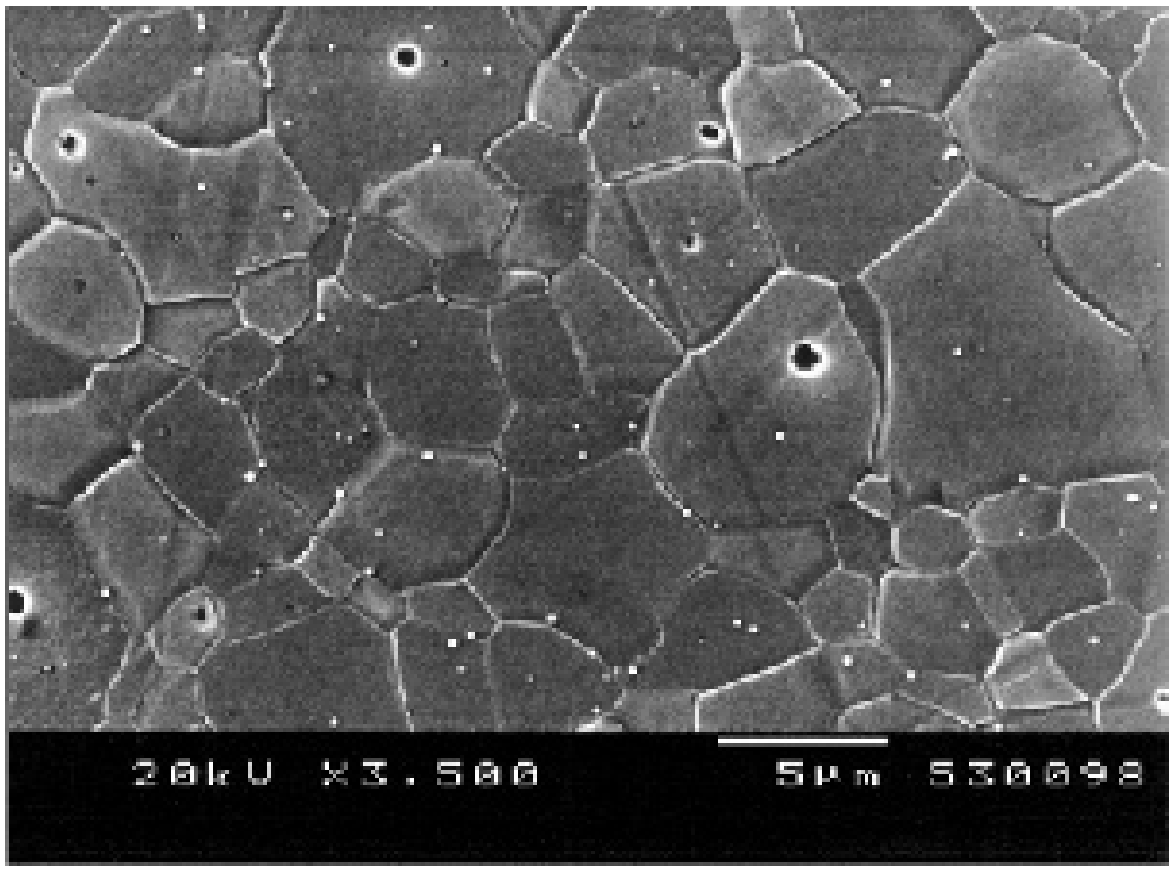

(c)

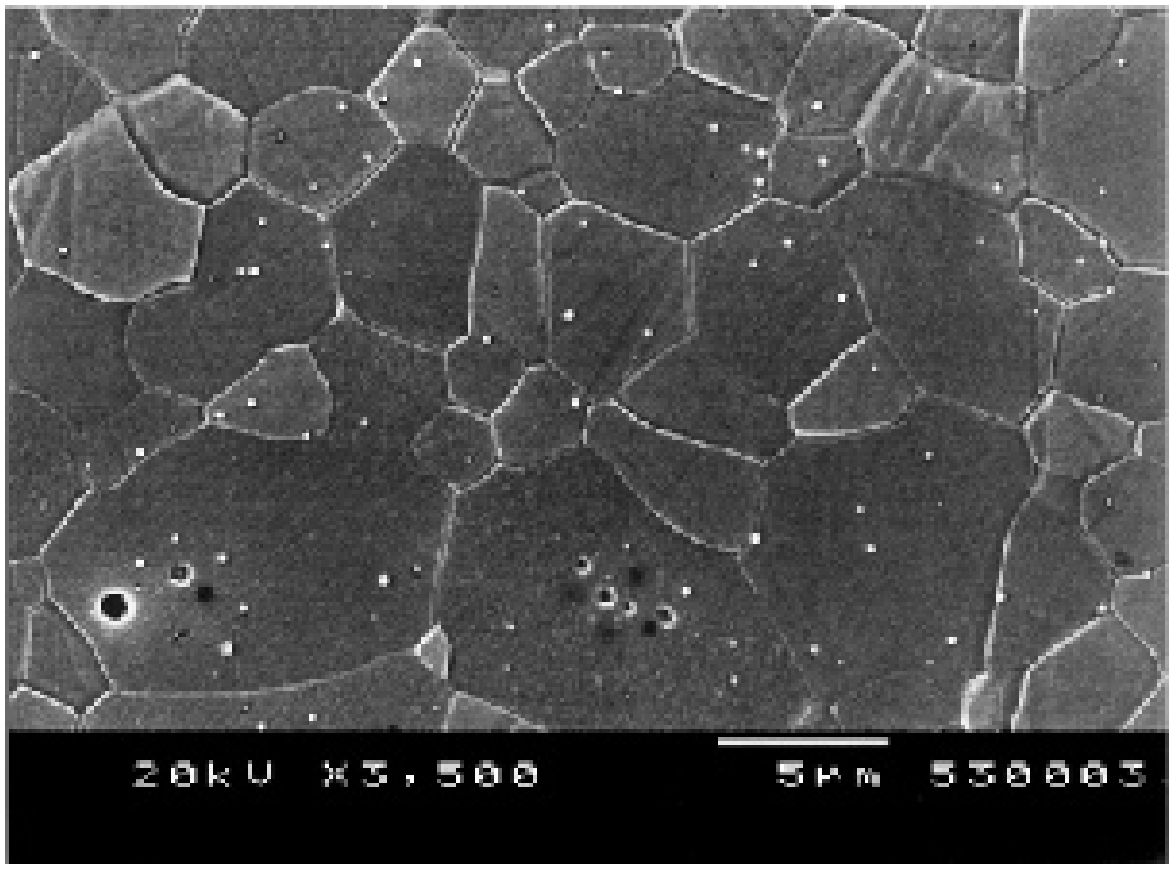

(d)

Figure 7 (*Continued*).

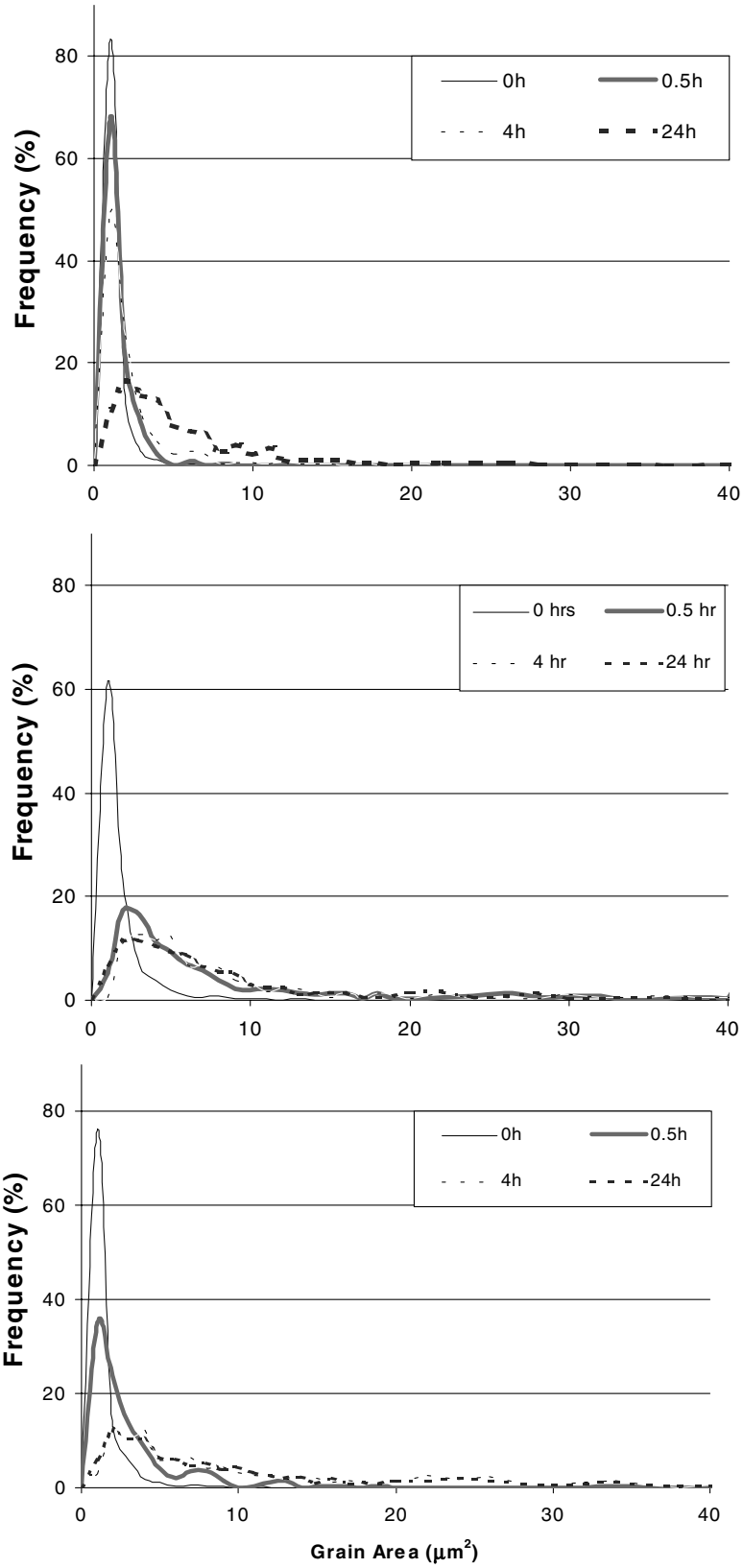

Figure 8 Grain size distributions of HA sintered in (a) air, (b) carbon dioxide, and (c) carbon dioxide with 3.2 kPa water.

HA ceramic sintered in air was undetectable whereas ceramics sintered in carbon dioxide atmospheres were all translucent to some degree. Fig. 9 shows the variation of optical transmission as a function of water partial pressure in carbon dioxide and sintering time at 1300°C. It can be seen that for all carbon dioxide atmospheres, maximum transmission was observed after four hours sintering and thereafter decreased considerably.

3.7. Infrared spectroscopy

FTIR showed that carbonate ions were present in the HA sintered in all carbon dioxide atmospheres at all

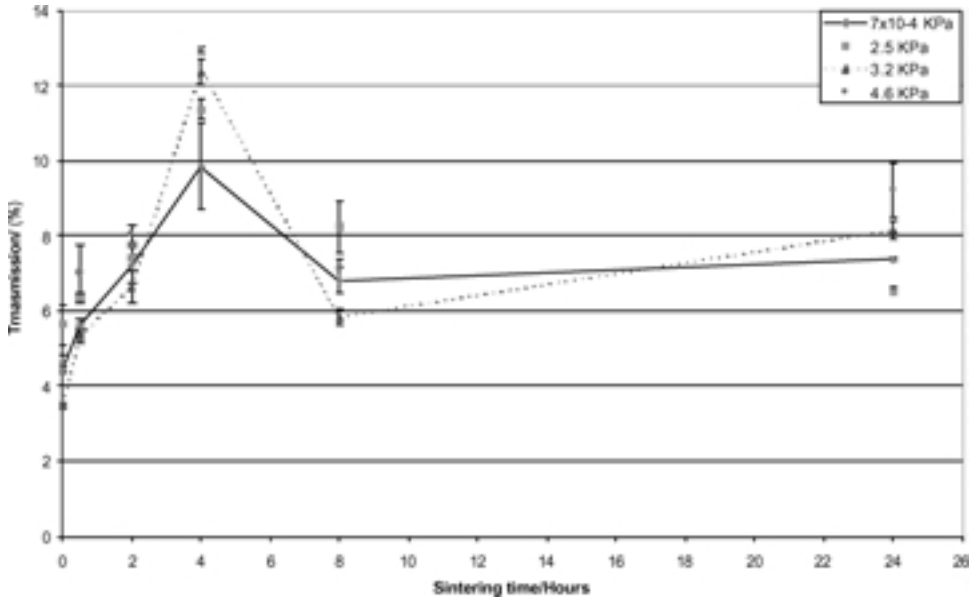

Figure 9 Optical transmission of HA sintered in carbon dioxide atmospheres as a function of sintering time.

timepoints. The intensity of the ν_3 carbonate peaks relative to the ν_3 phosphate peaks was higher in the HA sintered in carbon dioxide than the starting powder. Fig. 10a and b show the FTIR spectra of HA sintered in dry carbon dioxide and carbon dioxide with a water partial pressure of 4.6 kPa respectively at 1300°C for the times investigated.

Although water in the carbon dioxide atmosphere increased carbonate peak intensity relative to the phosphate peaks, little difference in the relative intensity of the various ν_3 carbonate peaks was observed Essentially four carbonate ν_3 peaks were observed; 1540, 1464, 1455 (doublet) and 1413 cm^{-1}. Peaks at 1540, and 1410 cm^{-1} have been assigned to carbonate located in the phosphate site (B-type) whereas 1550 and 1460 cm^{-1} have been assigned to hydroxyl substitution (A-type) [23]. The assignment of 1465 and 1455 cm^{-1} to A and B type substitutions respectively [24], does not help clarify the nature of the carbonate location, furthermore carbonate ν_2 peaks were invariably located at ~880 cm^{-1} which is closer to A type assignments of these previous studies than B type. On this basis it is believed that the material was probably a mixed A/B substitution. Small variations were observed with increasing sintering time; the intensity of the peak at ~1410 cm^{-1} (believed to be B type) diminished slightly after sintering times of 30 min and two hours in carbon dioxide and at 8 h in carbon dioxide/water and then returned to a similar intensity as at previous time points.

3.8. X-ray diffraction

Comparisons of X-ray diffraction data with JCPDS standards revealed that HA sintered in air for twenty-four hours did decompose slightly to produce a small quantity of tetracalcium phosphate. HA sintered in dry carbon dioxide decomposed to form a small quantity of tricalcium phosphate. At all other times and at all sintering times investigated in wet carbon dioxide the ceramic appeared to be phase pure hydroxyapatite. The effect of sintering time on the lattice parameters of HA sintered in carbon dioxide/water vapour at 1300°C is presented in Table III with lattice parameters of HA sintered for twenty-four hours in dry CO_2 and air. The **a** parameter increased during a sintering cycle with no dwell in carbon dioxide water mixture. After four hours and twenty-four hours sintering the **a** lattice parameter was more similar to that of the starting powder. After 4 h sintering the **c** parameter appeared to increase slightly and after sintering for twenty-four hours was more similar values to that at previous sintering times. However when sintered in carbon dioxide only for twenty-four hours both the **a** and **c** axes expanded compared to the starting material, whilst the same thermal treatment in air resulted in little change in **a** or **c** axes.

TABLE III The effect of sintering time and atmosphere on the lattice parameters of HA sintered at 1300°C for up to 24 h

Condition	**a** (=b)/Å	**c**/Å	R_{wp} (%)	R_p (%)	χ^2
Raw	9.4183 (1)	6.8868 (1)	1.98	1.46	2.00
CO_2/H_2O—0 h	9.4235 (1)	6.8874 (1)	2.92	1.96	4.47
CO_2/H_2O—4 h	9.4185 (1)	6.8905 (1)	2.46	1.71	3.20
CO_2/H_2O—24 h	9.4171 (1)	6.8828 (1)	2.89	1.93	4.23
CO_2—24 h	9.4252 (1)	6.8985 (1)	3.32	2.09	5.72
Air—24 h	9.4108 (1)	6.8861 (1)	3.15	2.05	5.33

3.9. Thermogravimetric analysis

In order to attempt to determine the carbonate content at different sintering times TGA was performed after dehydration until no weight loss was detected. Table IV shows that the starting material contained 2.9% carbonate. In carbon dioxide atmospheres less carbonate appeared to be lost than in air and most was retained in a carbon dioxide/water atmosphere. In this atmosphere carbonate appeared to be entering the structure during sintering at 1300°C. In other atmospheres investigated, little change occurred in carbonate content with

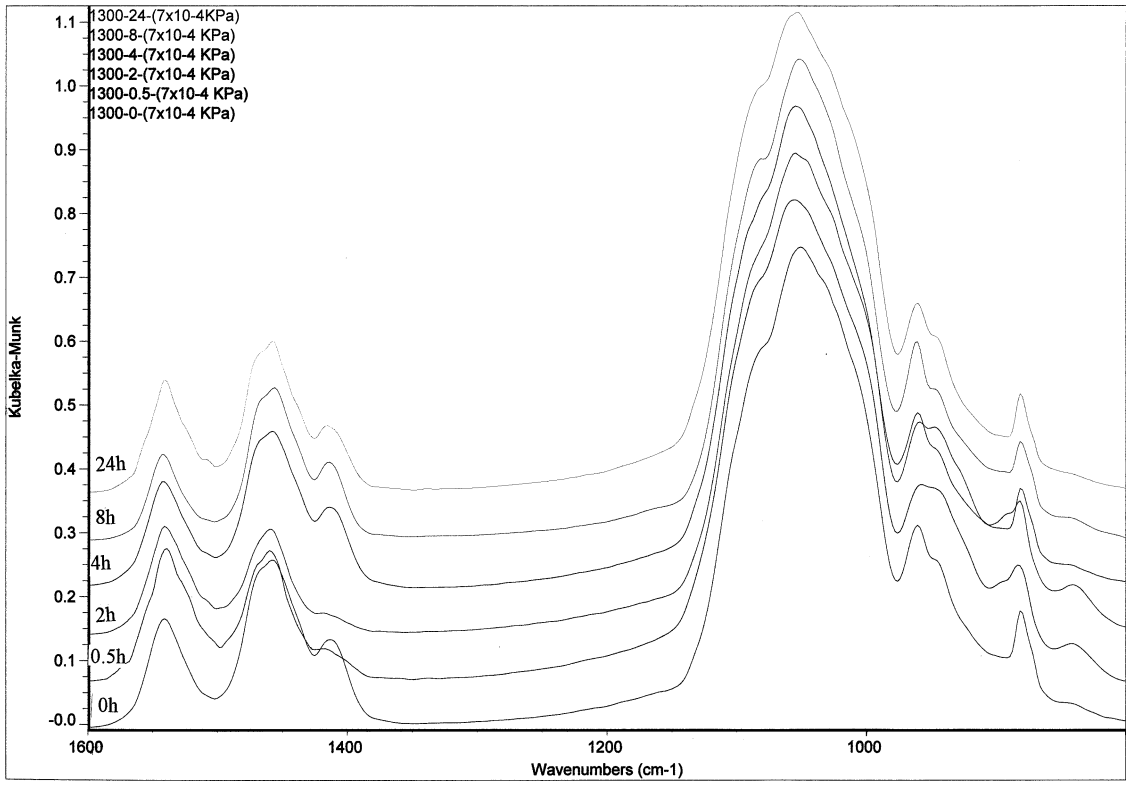

(a)

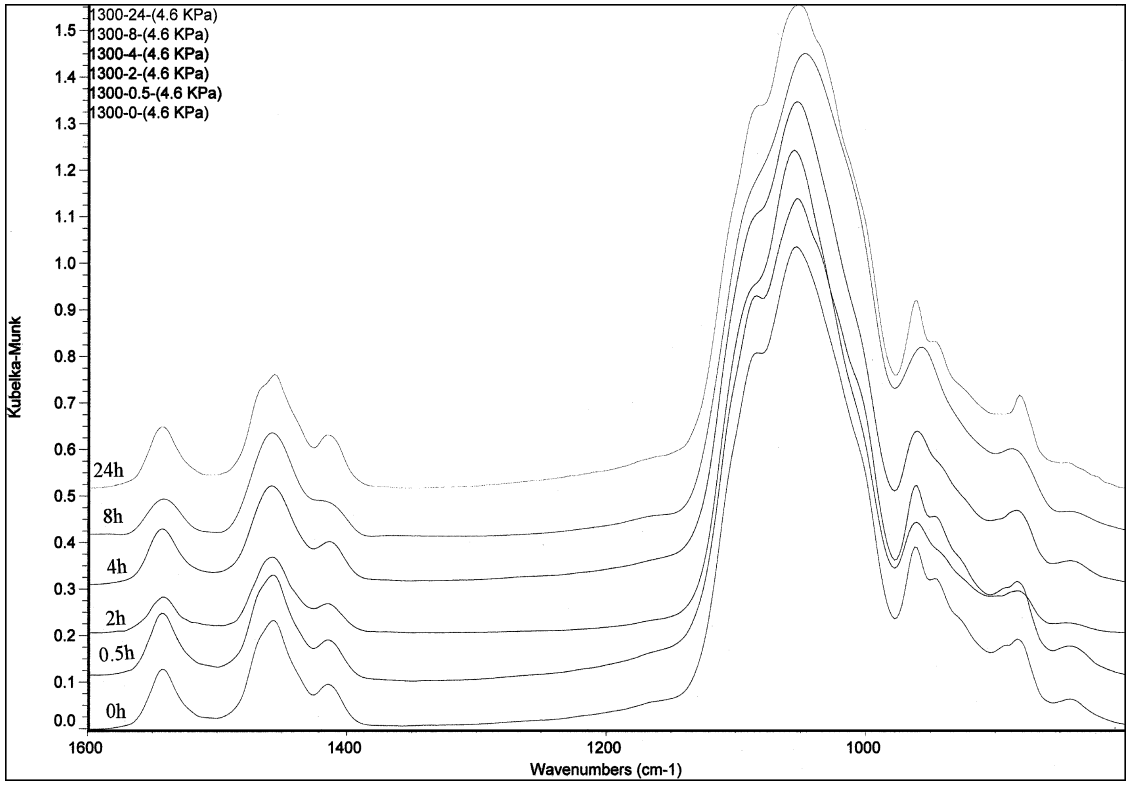

(b)

Figure 10 FTIR spectra of HA sintered in (a) carbon dioxide and (b) carbon dioxide and 4.6 kPa water at 1300°C for up to 24 h.

sintering time, though carbonate loss occurred during heating to 1300°C.

4. Discussion

Table I shows that potassium acetate and sodium orthophosphate appeared to decrease and increase the water content of the furnace atmosphere respectively compared with water alone. However there was large variability in these results that may have been caused by slight variation in room temperature or flow rate, hence this method would not appear suitable as a means of accurately controlling water content at the flow rates used since equilibrium conditions could

TABLE IV TGA data for starting powder, HA sintered at 1300°C in air, carbon dioxide and carbon dioxide with 4.6 kPa water

Time (h)\ atmosphere	Starting powder	CO_2	$CO_2 + 4.6$ kPa H_2O	Air
0	2.9%	0.75	0.8	0.4
24	–	0.6	1.55	0.32

not be reached. Lower flow rates may prove more successful.

Sintering data showed that carbon dioxide increased the temperature at which densification commenced, yet the densification rate was fastest in this atmosphere, as was grain growth rate was highest in this atmosphere; however, decomposition into βTCP occurred after prolonged sintering times. Manufacturer's data reported the Ca/P ratio as being 1.72, in which case CaO would be the expected decomposition product [25]. But previous work has shown that a carbonate apatite containing nearly 8 wt% carbonate which had a similar Ca/P ratio (1.71) also decomposed into βTCP at 1300°C in carbon dioxide atmospheres [26]. This suggests that carbonate containing HA has increased stability in carbon dioxide atmosphere over a range of carbonate contents. The decrease in density of HA ceramic sintered in carbon dioxide with sintering time as shown in Fig. 3 suggests that bloating of the ceramic may have occurred as a result of gas evolution. Pore size measurements confirmed that pore size did increase with sintering time.

The addition of water to the sintering atmosphere had the effect of reducing the temperature at which densification commenced and also reduced the sintering rate. Although no significant effect on mean grain size was observed, grain size distribution data showed that the presence of water in the sintering atmosphere delayed the onset of grain coarsening at 1300°C. HA sintered in air clearly had a smaller grain size than that sintered in carbon dioxide atmospheres. Although translucency has been reported in hydroxyapatite ceramics with fine grain size using HIP [27], another report also investigating HIP indicated that transparent HA ceramics were formed in the grain size range 5–10 μm [18]. The dependence of optical transmission on pore density and size is well known [28]. Generally ceramics in which measurable transmission was observed, demonstrated increased transmission as pore density decreased, however this was not always the case in our system, particularly for HA sintered for four hours. This implies that while pore density was important in determining translucency other factors may have also affected this property. The number of boundaries per unit length is proportional to linear grain dimension and Fig. 11 shows the relationship between optical transmission and grain size of the HA sintered in carbon dioxide atmospheres. There was an approximately linear relationship between transmission and grain size up to a limiting grain size of 4.3 μm, thereafter little relationship exists between them.

Even after twenty-four hours sintering in air, the grain size of the HA ceramic was only 2.5 μm. Certainly ceramics with the highest optical transmission in this

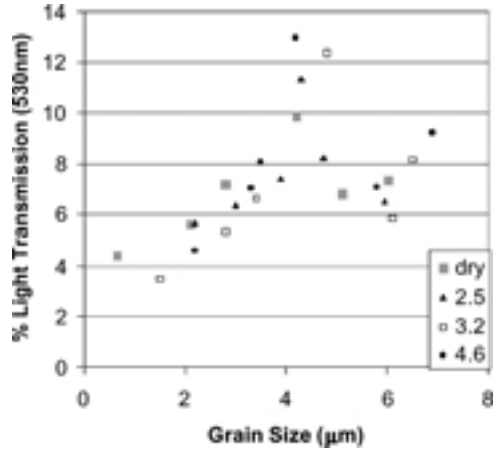

Figure 11 Optical transmission of HA as a function of grain size.

study did have microstructures containing of grains in that size range. As light is scattered by impurities such as pores and grain boundaries, increasing the grain size reduces the number of boundaries per unit length of the ceramic and hence should increase optical transmission. HA ceramics produced in air had a high pore density compared with ceramics sintered in carbon dioxide, furthermore the pore size in these ceramics would have caused maximal scattering due to their similarity with the wavelength of light used when sintered at two and four hours.

The P201 powder batch used in this study had a specific surface area of 21.7 $m^2\ g^{-1}$, however, preliminary work performed by us used P120 batch that had a SSA of 13.4 $m^2\ g^{-1}$ (manufacturer's data) and both batches produced ceramics with similar translucency in carbon dioxide atmospheres. The microcrystalline powder compacts used in this study did not form translucent ceramics after sintering in air, but only in carbon dioxide atmospheres at 1300°C. The maximum transmission of 2 mm thick ceramics was ~13% after 4 h sintering, shorter and longer sintering times resulted in less translucent ceramics (~3–9% transmission). Contrary to what might be expected form previous work on translucent and transparent apatite sintered using HIP, optical transmission appeared to be independent of relative density. However, calculations of ceramic relative density may have been inaccurate since HA density may have altered possibly as a result of compositional changes.

HA sintered in dry CO_2 decomposed into a mixture of HA and βTCP after twenty-four hours, however the presence of water inhibited this decomposition as has been observed previously [26]. Despite the phase stability of HA sintered in wet carbon dioxide Rietveld analysis of XRD patterns did show that variations in lattice parameters occurred with prolonged sintering. After 8 h sintering in carbon carbon dioxide/water, the B type carbonate peak in FTIR spectra at 1410 cm^{-1} decreased in intensity and then returned to similar levels as observed at shorter sintering times, otherwise little change in spectra were observed. The lattice parameters of the HA sintered in this condition did show temporal changes; the **a** axis increasing during the heating ramp to 1300°C and then decreasing again, the **c** axis

showed similar behaviour but after 4 h sintering. A type carbonate substitution has been associated with an increase in **a** axis and a decrease in **c** axis, [23], whilst the converse has been attributed B type substitution [29]. TGA showed that HA sintered in wet carbon dioxide lost carbonate during heating to 1300°C and then gained carbonate after sintering for twenty-four hours. It seems feasible that the initial **a** axis expansion may have occurred as B site carbonate moved to the A site as it left the structure [30], whilst the **c** axis expansion may have been a result of subsequent additional B type substitution from the sintering atmosphere. The lack of any clear changes in carbonate IR band position and intensity may have been due to the small changes involved or lattice parameter changes may have occurred as a result of a different structural change, e.g., loss of water [31].

5. Conclusion

Translucent HA ceramic may be formed from microcrystalline powder pressed compacts sintered at ambient pressure in carbon dioxide atmospheres, and optical transmission is at a maximum after four hours sintering at 1300°C. Carbon dioxide atmosphere enhanced grain growth and the elimination of fine pores, which is thought to be the reason for translucency of HA sintered in these atmospheres. The presence of water in carbon dioxide atmospheres appeared to reduce bloating of the HA after sintering for more than four hours. The reason why optical transmission appeared to decrease in ceramics sintered for longer than 4 h was not determined, however slight structural variation in either the HA lattice or the grain boundaries may have also affected optical transmission.

Acknowledgements

The authors wish to thank Mr. G. Dolman and Mr. R. Skeldon for their invaluable technical assistance with dilatometry and sintering.

References

1. H. AOKI, "Science and Medical Applications of Hydroxyapatite" (Takayama Press System Center Co., Tokyo, 1991) p. 5.
2. H. AOKI, K. KATO and T. SOKAWA, *Reports of Inst. for Med. Dent. Engineering, TMDU Tokyo* **58** (1973) 113.
3. M. JARCHO, C. H. BOLEN, M. B. THOMAS, J. BOBICK, J. F. KAY and R. H. DOREMUS, *J. Mater. Sci.* **11** (1976) 2027.
4. E. LANDI, A. TAMPIERI, G. CELOTTI and S. SPRIO, *J. Euro. Ceram. Soc.* **20** (2000) 2377.
5. M. G. S. MURRAY, J. WANG, C. B. PONTON and P. M. MARQUIS, *J. Mater. Sci.* **30** (1995) 3061.
6. H. MONMA, S. UENO and T. KANAZAWA, *J. Chem. Tech. Biotechnol.* **31** (1981) 15.
7. J. E. BARRALET, S. BEST and W. BONFIELD, *J. Mater. Sci.: Mats in Med.* **11** (2000) 719.
8. N. O. ENGIN and A. C. TAS, *J. Euro. Ceram. Soc.* **19** (1999) 2569.
9. D. C. TANCRED, B. A. O. McCORMACK and A. J. CARR, *Biomaterials* **19** (1998) 2303.
10. J. E. BARRALET, M. AKAO, H. AOKI and H. AOKI, *J. Biomed. Mater. Res.* **49** (2000) 176.
11. J. A. GILLES, D. L. CARNES and A. S. WINDELER, *J. Endodont.* **20** (1994) 327.
12. G. BOULON, A. COLLOMBET, A. BRENIER, M. T. COHEN-ADAD, A. YOSHIKAWA, K. LEBBOU, J. H. LEE and T. FUKUDA, *Adv. Functional Mater.* **11** (2001) 263.
13. R. EL OUENZERFI, G. PANCZER, C. GOUTAUDIER, M. T. COHEN-ADAD, G. BOULON, M. TRABELSI-AYEDI and N. KBIR-ARIGUIB, *Optical Mater.* **16** (2001) 301.
14. M. NAGAI, T. SAEKI and T. NISHINO, *J. Amer. Ceram. Soc.* **73** (1990) 1456.
15. G. C. PETRUCELLI, E. Y. KAWACHI, L. T. KUBOTA and C. A. BERTRAN, *Anal. Commun.* **33** (1996) 227.
16. K. TAKIKAWA and M. AKAO, *J. Mater. Sci.: Mats. in Med.* **7** (1996) 439.
17. H. AOKI, "Medical Applications of Hydroxyapatite" (Ishiyaku Euroamerica Inc, Tokyo, 1994) p. 154.
18. J. LI and J. HERMANSSON, *Interceram.* **39** (1990) 13.
19. J. MAJLING, P. ZNAIK, A. PALOVA, S. SVETIK, S. KOVALIK, D. K. AGRAWAL and R. ROY, *J. Mater. Res.* **12** (1997) 198.
20. K. UEMATSU, M. TAKAGI, T. HONDA, N. UCHIDA and K. SAITO, *J. Amer. Ceram. Soc.* **72** (1989) 1476.
21. J. E. BARRALET, S. BEST and W. BONFIELD, *J. Mater. Sci.: Mats in Med.* **11** (2000) 719.
22. "The Merck Index," 11th ed. (Merck and Co. Inc., Rahaway, NJ, 1989) Misc-109.
23. R. Z. LeGEROS, O. R. TRAUTZ, E. KLEIN and J. P. LEGEROS, *Spec. Experim.* **25** (1969) 5.
24. M. NADAL, J. C. TROMBE, G. BONEL and G. J. MONTEL, *Chim. Phys.* **67** (1970) 1161.
25. J. C. MERRY, I. R. GIBSON, S. BEST and W. BONFIELD, *J. Mater. Sci.: Mats. in Med.* **9** (1998) 779.
26. J. E. BARRALET, J. C. KNOWLES, S. BEST and W. BONFIELD *J. Mater. Sci.: Mats. in Med.* **13** (2002) 529.
27. F. WAKAI, Y. KODAMA, S. SAKAGUCHI and T. NONAMI, *J. Amer. Ceram. Soc.* **73** (1990) 457.
28. W. D. KINGERY, H. R. BOWEN and D. R. UHLMANN, "Introduction to Ceramics" (John Wiley and Sons, New York, 1976) p. 672.
29. G. BONEL, *Ann. Chim.* **147** (1972) 127.
30. R. A. YOUNG and D. W. HOLCOMBE, *Calcif. Tiss. Int.* **31** (1980) 189.
31. J. C. ELLIOTT, "Structure and Chemistry of the Apatites and Other Calcium Orthophosphates" (Elsevier, Amsterdam, 1994) p. 129.

Received 12 November 2002
and accepted 7 July 2003